

Microscopic quantum interference in excitonic condensation of Ta₂NiSe₅

Koudai Sugimoto,¹ Tatsuya Kaneko,² and Yukinori Ohta²

¹Center for Frontier Science, Chiba University, Chiba 263-8522, Japan

²Department of Physics, Chiba University, Chiba 263-8522, Japan

(Received 21 October 2015; published 15 January 2016)

The microscopic quantum interference associated with excitonic condensation in Ta₂NiSe₅ is studied in a BCS-type mean-field approximation. We show that in ultrasonic attenuation the coherence peak appears just below the transition temperature T_c , whereas in NMR spin-lattice relaxation the rate rapidly decreases below T_c ; these observations can offer a crucial experimental test for the validity of the excitonic condensation scenario in Ta₂NiSe₅. We also show that excitonic condensation manifests itself in a jump of the heat capacity at T_c as well as in a softening of the elastic shear constant, in accordance with the second-order phase transition observed in Ta₂NiSe₅.

DOI: [10.1103/PhysRevB.93.041105](https://doi.org/10.1103/PhysRevB.93.041105)

A prediction was made about half a century ago that, in a semimetal or a narrow-gap semiconductor, electrons in a conduction band (CB) and holes in a valence band (VB) form pairs called excitons, and the system spontaneously goes into a state of quantum condensation with macroscopic phase coherence [1–7]. The state leads to the opening of a band gap in semimetals or to the flattening of the band edges in semiconductors, and is called the excitonic insulator state. The phase of such states may generally be referred to as the excitonic phase. A recent development in experimental techniques, in particular, angle-resolved photoemission spectroscopy (ARPES), enables one to observe the changes in the band structure due to possible excitonic condensation in some materials [8–12]. Thereby, the excitonic phases have attracted renewed attention in recent years [13].

Here, we focus on a candidate material Ta₂NiSe₅ [11], which is a narrow-gap semiconductor undergoing a structural transition from an orthorhombic to monoclinic phase at $T_c = 328$ K [14,15]. The flat band was observed in the ARPES experiment [11,12,16], which was interpreted to be due to excitonic condensation; i.e., a mean-field analysis of the proposed three-chain Hubbard model with electron-phonon coupling explains the simultaneous occurrence of excitonic condensation and structural transition [17], and a variational-cluster-approximation calculation of the extended Falicov-Kimball model well reproduces the ARPES spectral weight observed experimentally [16]. However, a “smoking gun” experiment that determines whether Ta₂NiSe₅ is really in the excitonic phase is still lacking.

In this Rapid Communication, we challenge this issue; i.e., we will argue that the presence/absence of the coherence peak caused by microscopic quantum interference in the state can provide a crucial experimental test for the validity of the excitonic condensation scenario in this material. In the case of superconductivity, it is known that the coherence factors appearing in ultrasonic attenuation and nuclear-magnetic-resonance (NMR) relaxation rates played an essential role in confirming the validity of the BCS theory [18,19]. We apply this concept to the case of excitonic phases, whose state can be written in terms of a BCS-type wave function as well. We thereby present how the microscopic quantum interference of the state can give rise to either a coherence peak or a rapid decrease in the temperature dependence of these rates, of which

not much is known so far, except for a simple model calculation of the ultrasonic attenuation rate [20,21].

In what follows, we will first introduce a three-chain Hubbard model with electron-phonon coupling that describes the low-energy electronic states of Ta₂NiSe₅, and present some generalization of the mean-field calculations of Kaneko *et al.* [17], demonstrating an excitonic and structural phase transition [22]. We will then calculate the temperature dependence of the ultrasonic attenuation and NMR spin-lattice relaxation rates and demonstrate that the coherence peak appears in the ultrasonic attenuation rate due to constructive interference, while there occurs a rapid decrease in the NMR relaxation rate due to destructive interference, the behaviors of which are in contrast to those of BCS *s*-wave superconductivity. We will also carry out the calculations of thermodynamic quantities, such as heat capacity and elastic constant, and show that a jump is observed in the specific heat at the phase transition and that elastic softening relating to the structural phase transition is observed in the elastic shear constant. Our theoretical predictions are in fair agreement with available experimental data obtained so far for Ta₂NiSe₅, which we hope will encourage further experimental studies to provide the proof that Ta₂NiSe₅ is in the excitonic phase.

To be quantitative, let us introduce the three-chain Hubbard model with electron-phonon coupling used in Ref. [17], which consists of a doubly degenerate CB of two Ta *5d* chains and a nondegenerate VB of a Ni *3d* chain, as is illustrated schematically in Fig. 1. We define $c_{j,\alpha,\sigma}$ ($c_{j,\alpha,\sigma}^\dagger$) to be an annihilation (creation) operator of a CB electron at site j with spin σ on the chain α ($= 1, 2$) and $f_{j,\sigma}$ ($f_{j,\sigma}^\dagger$) to be an annihilation (creation) operator of a VB electron at site j with spin σ . It was shown [17,22] that the BCS-type mean-field approximation to this model successfully describes the simultaneous occurrence of excitonic condensation and structural transition from the orthorhombic to monoclinic phase of Ta₂NiSe₅. The diagonalized mean-field Hamiltonian \mathcal{H}^{MF} reads

$$\mathcal{H}^{\text{MF}} = \sum_{k,\sigma} \sum_{\epsilon=c,\pm} E_{k,\epsilon} \gamma_{k,\epsilon,\sigma}^\dagger \gamma_{k,\epsilon,\sigma} + N\epsilon_0, \quad (1)$$

where $E_{k,\epsilon,\sigma}$ is the quasiparticle energy, $\gamma_{k,\epsilon,\sigma}$ ($\gamma_{k,\epsilon,\sigma}^\dagger$) is an annihilation (creation) operator of the quasiparticle with

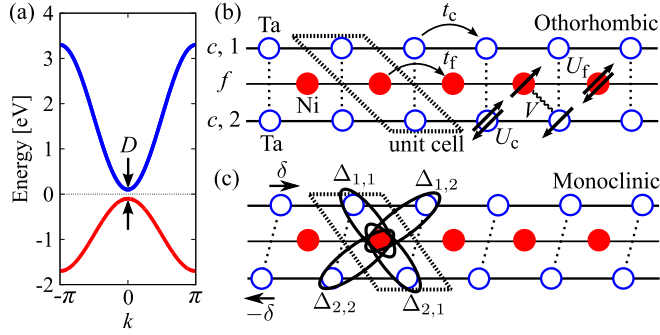


FIG. 1. (a) Noninteracting band structure of our model with hopping parameters $t_c = -0.8$ and $t_f = 0.4$ eV and band gap $D = 0.2$ eV. Also shown are the schematic representations of the lattice structures of (b) the orthorhombic and (c) monoclinic phases. We assume the on-site Coulomb repulsion U_c on c and U_f on f sites and intersite Coulomb repulsion V between the c and f sites. We set $V = 0.6$ eV and $U_c = U_f = 4$ V. The electron-phonon coupling of strength $\lambda = 0.01$ eV is assumed unless otherwise stated. The order parameters are defined for the excitonic condensation as $\Delta_{\alpha,\beta}$ and for the structural distortion as δ .

band index ϵ , wave number k , and spin σ , and $N\epsilon_0$ is a constant term in the mean-field Hamiltonian. N is the number of the unit cells in the system. The quasiparticle satisfies $c_{k,\mu,\sigma} = \sum_{\epsilon} \psi_{k,\sigma;\mu,\epsilon} \gamma_{k,\epsilon,\sigma}$, where $\psi_{k,\sigma;\mu,\epsilon}$ is the Bogoliubov transformation coefficient and $f_{k,\sigma} = c_{k,3,\sigma}$. Details of our mean-field analysis are given in the Supplemental Material [22].

First, let us discuss the ultrasonic attenuation rate. Defining $A_{q,\alpha} = a_{q,\alpha} + a_{-q,\alpha}^\dagger$ using the phonon annihilation (creation) operator $a_{q,\alpha}$ ($a_{q,\alpha}^\dagger$) on the Ta chain α , we write the Matsubara phonon Green's function as

$$D_{\alpha}(q, \tau) = -\langle T_{\tau} A_{q,\alpha}(\tau) A_{-q,\alpha}(0) \rangle, \quad (2)$$

where $A_{q,\alpha}(\tau) = e^{-\omega_q \tau} a_{q,\alpha} + e^{\omega_q \tau} a_{-q,\alpha}^\dagger$ is the Heisenberg representation of $A_{q,\alpha}$ at imaginary time τ and phonon wave number q with a phonon dispersion ω_q . Using the Fourier coefficient $\mathcal{D}_{\alpha}(q, i\omega_n) = \int_0^{\beta \hbar} d\tau \mathcal{D}_{\alpha}(q, \tau) e^{i\omega_n \tau}$, the phonon Dyson's equation is given as

$$\mathcal{D}_{\alpha}(q, i\omega_n) = \mathcal{D}_{\alpha}^{(0)}(q, i\omega_n) + \mathcal{D}_{\alpha}^{(0)}(q, i\omega_n) \Pi_{\alpha}(q, i\omega_n) \times \mathcal{D}_{\alpha}(q, i\omega_n), \quad (3)$$

where $\Pi_{\alpha}(q, i\omega_n)$ is the self-energy of the phonon Green's function. The ultrasonic attenuation rate is then given by the imaginary part of the retarded self-energy [23] as

$$\alpha_{q,\alpha} = \frac{1}{\tau_{q,\alpha}} = -2 \text{Im} \Pi_{\alpha}^R(q, \omega_q + i\eta), \quad (4)$$

where $\tau_{q,\alpha}$ is a relaxation time of the phonon and η is an infinitesimal value.

We consider the lattice oscillation corresponding to the distortion in the structural phase transition, i.e., an ultrasonic shear wave for the transverse acoustic mode that propagates along the direction perpendicular to the chains [see Fig. 2(d)]. The perturbation Hamiltonian of the phonons coupled with

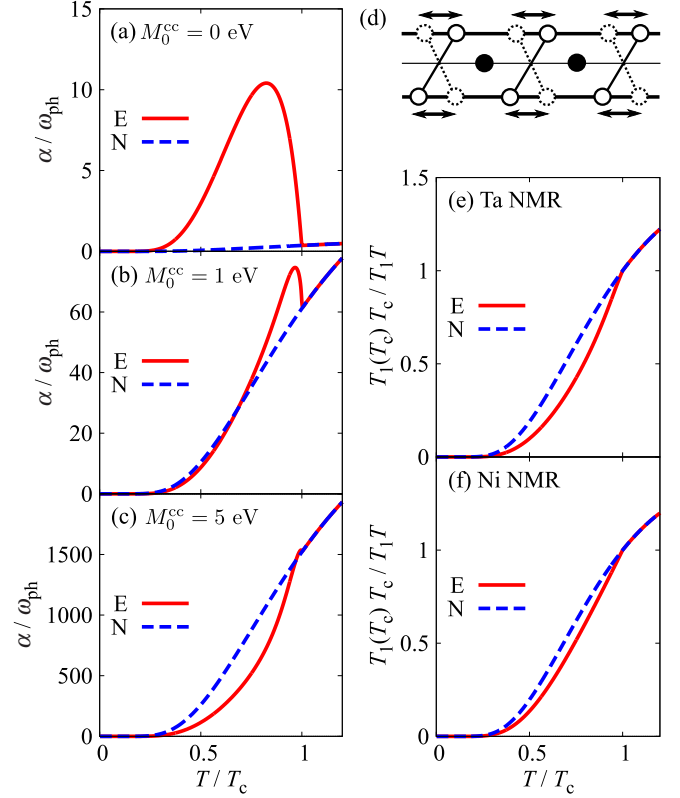


FIG. 2. Calculated ultrasonic attenuation rate normalized by the ultrasonic frequency ω_{ph} . We assume $M_0^{\text{cf}} = 1$ eV with (a) $M_0^{\text{cc}} = 0$ eV, (b) $M_0^{\text{cc}} = 1$ eV, and (c) $M_0^{\text{cc}} = 5$ eV. (d) Schematic representation of the oscillation of the ultrasonic shear wave that propagates along the direction perpendicular to the chains. Also shown are the calculated NMR relaxation rates at (e) Ta and (f) Ni sites. The red solid line (E) is for the excitonic phase and the blue dashed line (N) is for the normal phase.

electrons is given by

$$\mathcal{H}' = \sum_{k,q,\sigma} \sum_{\alpha=1}^2 \left\{ M_{-q}^{\text{cc}} A_{-q,\alpha} c_{k-,\alpha,\sigma}^\dagger c_{k+,\alpha,\sigma} - M_{-q}^{\text{cf}} A_{-q,\alpha} (c_{k-,\alpha,\sigma}^\dagger f_{k+,\sigma} + f_{k-,\alpha,\sigma}^\dagger c_{k+,\sigma}) \right\}, \quad (5)$$

with $k_{\pm} = k \pm \frac{q}{2}$. The first term represents the coupling between the phonon and charge density of the CB electrons with a coupling constant M_{-q}^{cc} , and the second term represents the hybridization between the conduction and valence bands by the phonon with a coupling constant $M_{-q}^{\text{cf}} = \sqrt{\frac{K\lambda\hbar}{M_c\omega_q}}$, where M_c is the mass of a Ta ion, K is the spring constant of the lattice harmonic oscillators, and λ is the electron-phonon coupling strength [17,22]. The coupling between the phonon and charge density of the VB electrons is ignored as being irrelevant to the present instability mode. Equation (5) then reads

$$\mathcal{H}' = \sum_{k,q,\sigma} \sum_{\alpha=1}^2 \sum_{\mu=1}^3 W_{\alpha,\mu}(-q) A_{-q,\alpha} \times (c_{k-,\alpha,\sigma}^\dagger c_{k+,\mu,\sigma} + c_{k-,\mu,\sigma}^\dagger c_{k+,\alpha,\sigma}), \quad (6)$$

with $W_{\alpha,\mu}(q) = (\frac{1}{2}M_q^{cc}\delta_{\alpha,\mu} - M_q^{cf}\delta_{\mu,3})$.

We adopt the second-order perturbation theory for the phonon self-energy. Since the ultrasonic wave number q is small enough, we may assume $q \simeq 0$ in Eq. (4). We then obtain

$$\begin{aligned} \alpha_{q=0,\alpha} &= 2\pi\omega_{\text{ph}} \sum_{k,\sigma} \sum_{\epsilon_1,\epsilon_2} \frac{\beta}{4 \cosh^2[\beta(E_{k,\epsilon_1} - \mu)/2]} \\ &\times \delta(E_{k,\epsilon_1} - E_{k,\epsilon_2}) \sum_{\mu,\nu} W_{\alpha,\mu} W_{\alpha,\nu} \{2\Psi_{\alpha,\alpha;\epsilon_1}(k,\sigma) \\ &\times \Psi_{\mu,\nu;\epsilon_2}(k,\sigma) + \Psi_{\nu,\alpha;\epsilon_1}(k,\sigma)\Psi_{\mu,\alpha;\epsilon_2}(k,\sigma) \\ &+ \Psi_{\alpha,\mu;\epsilon_1}(k,\sigma)\Psi_{\alpha,\nu;\epsilon_2}(k,\sigma)\}, \end{aligned} \quad (7)$$

with $\Psi_{\nu,\kappa;\epsilon}(k,\sigma) = \psi_{k,\sigma;\nu,\epsilon} \psi_{k,\sigma;\kappa,\epsilon}^*$ and the ultrasonic frequency ω_{ph} .

The calculated results for the temperature dependence of the ultrasonic attenuation rate are shown in Figs. 2(a)–2(c). We find the following: In the normal state (obtained with vanishing order parameters), thermally excited electrons are scattered by phonons via the coupling with charge density, resulting in the behavior $\alpha \propto (M_0^{cc})^2$. The M_0^{cf} term does not contribute here. In the excitonic phase, a large coherence peak appears due to the phonon-induced c - f hybridization (M_0^{cf}), which is, however, overwhelmed by the charge-density term (M_0^{cc}) at $M_0^{cc} \gg M_0^{cf}$, where the increase in the band gap suppresses the thermal excitation of electrons, resulting in a rapid decrease in the rate α . However, in the ultrasonic attenuation experiment using the transverse sound mode, the coupling between the phonon and charge density of electrons does not contribute to the rate, and therefore we have the situation shown in Fig. 2(a). The experimental observation of the coherence peak in the ultrasonic attenuation rate should thus be realizable.

Next, let us discuss the NMR spin-lattice relaxation rate, which may be written [24] as

$$\frac{1}{T_{1,\mu}} \propto -\frac{k_B T}{\hbar\omega_\mu} \sum_q \text{Im} \chi_{+-,\mu}^R(q, \omega_\mu), \quad (8)$$

using the transverse dynamical spin susceptibility

$$\chi_{+-,\mu}^R(q, \omega_\mu) = -i \int_{-\infty}^{\infty} dt e^{i\omega_\mu t} \langle [S_{q,\mu}^+(t), S_{-q,\mu}^-(0)] \theta(t) \rangle, \quad (9)$$

where we define $S_{q,\mu}^+ = \sum_k c_{k-,\mu,\uparrow}^\dagger c_{k+,\mu,\downarrow}$ and $S_{q,\mu}^- = \sum_k c_{k-,\mu,\downarrow}^\dagger c_{k+,\mu,\uparrow}$, and ω_μ is a resonant frequency of nuclear spins ($\mu = 1, 2$ for Ta and $\mu = 3$ for Ni). Using the mean-field approximation and assuming a small ω_μ value compared to typical energy scales of the system, we may rewrite Eq. (8) as

$$\begin{aligned} \frac{1}{T_{1,\mu}} &\propto \pi \sum_{k,q} \sum_{\epsilon_1,\epsilon_2} \Psi_{\mu,\mu;\epsilon_1}(k-, \uparrow) \Psi_{\mu,\mu;\epsilon_2}(k+, \downarrow) \\ &\times \frac{1}{4 \cosh^2[\beta(E_{k-,\epsilon_1} - \mu)/2]} \delta(E_{k-,\epsilon_1} - E_{k+,\epsilon_2}). \end{aligned} \quad (10)$$

The calculated results for the temperature dependence of the NMR relaxation rate are shown in Figs. 2(e) and 2(f) for Ta and Ni nuclear spins, respectively. We find that, in contrast to the typical s -wave superconducting phase [19], there appear

no characteristic peaks in the rate of the excitonic phase but the rate simply drops just below T_c . Thus, the behavior of the NMR relaxation rate in the excitonic phase is similar to that of an ultrasonic attenuation rate in the s -wave superconducting phase. We point out that a recent NMR experiment on Ta_2NiSe_5 [25] suggests the behavior of the rate consistent with our theoretical prediction.

Here, we briefly mention the nuclear-quadrupole-resonance (NQR) relaxation rate. We first note that the quadrupole interaction in NQR is the BCS case I interaction (without spin-flip processes) [26] while the spin-lattice relaxation in NMR is the BCS case II interaction (with spin-flip processes) [18,27]. Because the electron-phonon interaction in the ultrasonic attenuation is the case I interaction as well, we may expect that the NQR relaxation rate should behave similarly with the ultrasonic attenuation rate where the coherence peak rapidly grows below T_c , as we have shown above. However, because the nuclear-quadrupole interaction comes not only from the on-site anisotropic charge distribution (which does not cause the coherence peak) but also from the intersite quadrupole interaction and the latter is not easy to evaluate, here we only suggest the possibility that the coherence peak can appear in the NQR relaxation rate, just as in the ultrasonic attenuation rate shown in Figs. 2(a)–2(c). Experimental studies are desired.

Finally, let us demonstrate that the excitonic condensation manifests itself in some thermodynamic quantities, such as heat capacity and elastic constant, which will provide additional experimental support for the validity of the excitonic condensation scenario in Ta_2NiSe_5 . Let us first discuss the heat capacity, which may be calculated from the mean-field free energy [22] as

$$C = -T \frac{\partial^2 F}{\partial T^2} = \sum_{k,\epsilon,\sigma} (E_{k,\epsilon} - \mu) \frac{\partial f(E_{k,\epsilon})}{\partial T}, \quad (11)$$

where $f(E)$ is the Fermi distribution function. The calculated result is shown in Fig. 3(a), where we find that the jump at T_c associated with the second-order phase transition is clearly visible, satisfying the entropy balance. The jump is given by $(C_E - C_N)/C_N \simeq 0.20$ for the parameter values appropriate for Ta_2NiSe_5 , where C_E and C_N are the heat capacities in the excitonic and normal phases, respectively, at T_c . This value is much smaller than the value 1.43 (a universal constant) in the BCS superconductivity and depends strongly on the model parameters used; its λ dependence, e.g., is shown in Fig. 3(b). Such a difference in the magnitude of the jump comes mainly from the difference in the normal phase: It is a band insulator in the present excitonic condensation while it is a metal in superconductivity. We also note in Fig. 3(b) that the jump in the heat capacity and the value of T_c increase monotonically as λ increases, indicating that the larger values of the order parameters in the excitonic phase lead to the larger jump in the heat capacity. We point out that a recent specific heat measurement on Ta_2NiSe_5 [28] reveals a behavior consistent with our theoretical prediction.

The elastic shear constant may also be calculated from the mean-field free energy [22] as

$$C_{\text{shear}} = \frac{\partial^2 F}{\partial \delta^2}, \quad (12)$$

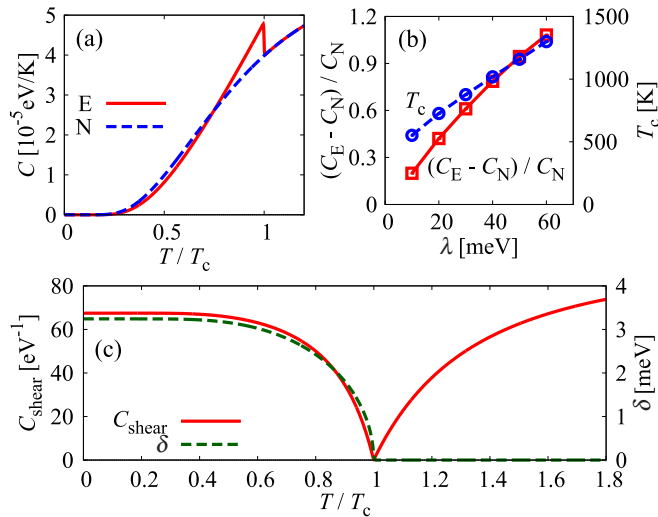


FIG. 3. (a) Calculated temperature dependence of the heat capacity per unit cell, where the red solid line is for the excitonic phase and the blue dashed line is for the normal phase. (b) Calculated λ dependence of the jump in the heat capacity (red squares) and T_c (blue circles). (c) Calculated temperature dependence of the elastic shear constant per unit cell (red solid line) and that of the lattice distortion δ (green dashed line).

where we assume the lattice distortion of the transverse acoustic phonon mode in the long wavelength limit, corresponding to the observed structural phase transition [see Fig. 2(d)]. The calculated result is shown in Fig. 3(c), where we actually find the elastic softening at T_c , leading to the structural phase transition. We observe a Curie-Weiss-like behavior $1/C_{\text{shear}} = 1/C_{\text{shear}}^\infty + A/(T - T_c)$ at $T > T_c$ with $1/C_{\text{shear}}^\infty = 0.094 \text{ eV}$ and $A = 0.546 \text{ eV K}$. A recent experimental observation of the diffuse x-ray scattering [29] suggests the presence of the

soft phonon mode, which is consistent with our theoretical prediction. The calculated lattice distortion δ at $T < T_c$ is also consistent with the observed temperature dependence of the monoclinic angle of the lattice [14].

In summary, we have studied the microscopic quantum interference associated with excitonic condensation in Ta_2NiSe_5 using the BCS-type mean-field approximation for the three-chain Hubbard model with electron-phonon coupling. We have calculated the temperature dependence of the ultrasonic attenuation and NMR relaxation rates, and have shown that the coherence peak can appear in the ultrasonic attenuation rate just below T_c . In the NMR relaxation rate, on the other hand, no characteristic peak appears in $1/T_1$ but it simply drops just below T_c , in agreement with recent NMR data for Ta_2NiSe_5 [25]. The direct observation of the coherence peak in the ultrasonic attenuation rate will then provide a crucial experimental test for the presence of the excitonic phase in Ta_2NiSe_5 . We have also demonstrated that the heat capacity exhibits a relatively small jump at T_c and the elastic shear constant indicates a softening when the temperature approaches T_c , both of which are consistent with recent experimental observations for Ta_2NiSe_5 [28,29]. We therefore hope that our theoretical predictions made here will encourage further experimental studies to provide proof that the excitonic condensation actually occurs in Ta_2NiSe_5 .

We thank M. Itoh, Y. Kobayashi, Y. F. Lu, K. Matsubayashi, T. Mizokawa, H. Sawa, and H. Takagi for discussing experimental aspects of Ta_2NiSe_5 and H. Fehske, H. Fukuyama, M. Ogata, and T. Toriyama for theoretical aspects. This work was supported in part by Grants-in-Aid for Scientific Research from JSPS (No. 26400349 and No. 15H06093) of Japan. T.K. acknowledges support from a JSPS Research Fellowship for Young Scientists.

- [1] N. F. Mott, *Philos. Mag.* **6**, 287 (1961).
- [2] R. S. Knox, in *Solid State Physics*, edited by F. Seitz and D. Turnbull (Academic Press, New York, 1963), Suppl. 5, p. 100.
- [3] L. V. Keldysh and Y. V. Kopaev, *Sov. Phys. Solid State* **6**, 2219 (1965).
- [4] J. des Cloizeaux, *J. Phys. Chem. Solids* **26**, 259 (1965).
- [5] D. Jérôme, T. M. Rice, and W. Kohn, *Phys. Rev.* **158**, 462 (1967).
- [6] B. I. Halperin and T. M. Rice, *Rev. Mod. Phys.* **40**, 755 (1968).
- [7] For a recent review, see J. Kuneš, *J. Phys.: Condens. Matter* **27**, 333201 (2015).
- [8] H. Cercellier, C. Monney, F. Clerc, C. Battaglia, L. Despont, M. G. Garnier, H. Beck, P. Aebi, L. Patthey, H. Berger, and L. Forró, *Phys. Rev. Lett.* **99**, 146403 (2007).
- [9] C. Monney, H. Cercellier, F. Clerc, C. Battaglia, E. F. Schwier, C. Didiot, M. G. Garnier, H. Beck, P. Aebi, H. Berger, L. Forró, and L. Patthey, *Phys. Rev. B* **79**, 045116 (2009).
- [10] C. Monney, G. Monney, P. Aebi, and H. Beck, *Phys. Rev. B* **85**, 235150 (2012).
- [11] Y. Wakisaka, T. Sudayama, K. Takubo, T. Mizokawa, M. Arita, H. Namatame, M. Taniguchi, N. Katayama, M. Nohara, and H. Takagi, *Phys. Rev. Lett.* **103**, 026402 (2009).
- [12] Y. Wakisaka, T. Sudayama, K. Takubo, T. Mizokawa, N. L. Saini, M. Arita, H. Namatame, M. Taniguchi, N. Katayama, M. Nohara, and H. Takagi, *J. Supercond. Novel Magn.* **25**, 1231 (2012).
- [13] T. Kaneko, B. Zenker, H. Fehske, and Y. Ohta, *Phys. Rev. B* **92**, 115106 (2015), and references therein.
- [14] F. J. Di Salvo, C. H. Chen, R. M. Fleming, J. V. Waszczak, R. G. Dunn, S. A. Sunshine, and J. A. Ibers, *J. Less-Common Met.* **116**, 51 (1986).
- [15] E. Canadell and M. H. Whangbo, *Inorg. Chem.* **26**, 3974 (1987).
- [16] K. Seki, Y. Wakisaka, T. Kaneko, T. Toriyama, T. Konishi, T. Sudayama, N. L. Saini, M. Arita, H. Namatame, M. Taniguchi, N. Katayama, M. Nohara, H. Takagi, T. Mizokawa, and Y. Ohta, *Phys. Rev. B* **90**, 155116 (2014).
- [17] T. Kaneko, T. Toriyama, T. Konishi, and Y. Ohta, *Phys. Rev. B* **87**, 035121 (2013); **87**, 199902(E) (2013).
- [18] J. Bardeen, L. N. Cooper, and J. R. Schrieffer, *Phys. Rev.* **108**, 1175 (1957).
- [19] L. C. Hebel and C. P. Slichter, *Phys. Rev.* **113**, 1504 (1959).
- [20] K. Maki and K. Nakanishi, *J. Low Temp. Phys.* **5**, 1 (1971).

- [21] R. E. Amritkar and N. Kumar, *Solid State Commun.* **26**, 627 (1978).
- [22] See Supplemental Material at <http://link.aps.org/supplemental/10.1103/PhysRevB.93.041105> for details of the mean-field calculations.
- [23] S. Hershfield and M. Y. Reizer, *Phys. Rev. B* **43**, 9475 (1991).
- [24] T. Moriya, *J. Phys. Soc. Jpn.* **18**, 516 (1963).
- [25] S. Lee, Y. Kobayashi, and M. Itoh (unpublished).
- [26] R. H. Hammond and W. D. Knight, *Phys. Rev.* **120**, 762 (1960).
- [27] M. Tinkham, *Introduction to Superconductivity* (McGraw-Hill, New York, 1975).
- [28] Y. F. Lu, H. Takagi *et al.* (unpublished).
- [29] N. Katayama and H. Sawa (private communication).